Aperito Online Publishing

Aperito Journal of Recent Trends in Genomics and Proteomics

Received: Oct 23, 2014
Accepted: Oct 03, 2014
Published: Oct 06, 2014

http://dx.doi.org/10.14437/AJRTGP-1-103 Research Pao-Chi Liao, Aperito J Recent Trends Genome Proteom 2014, 1:1

An Alternative of Phosphopeptide Identification using Inclusion List-Driven Targeted Liquid-Tandem Mass Spectrometry for Label-Free Quantitative Tyrosine Phosphoproteomics: Application of Src Inhibitor-Related Signaling Pathway Analyses in Lung Cancer

Ming-Chuan Wang[1,2], Eric S.L. Hsiaoa,[2], Yu-Chang Tyan[3,4,5], Tzu-Hsien Yang[6], Juo-Ling Sun[2], Hsin-Yi Wu[7], Wen-Chang Tseng[8], Yu-Ju Chen[7], Yeou-Guang Tsay[8], Sergei Moshkovskii [9], Yu-Chen Chang [2], Wei-Sheng Wu[6] and Pao-Chi Liao[*1,2]

[1]Proteomics Research Core Laboratory, College of Medicine, National Cheng Kung University, Tainan, Taiwan.

[2]Department of Environmental and Occupational Health, College of Medicine, National Cheng Kung University, Tainan, Taiwan

[3]Department of Medical Imaging and Radiological Sciences, Kaohsiung Medical University, 100 Shi-Chuan 1st Road, Kaohsiung 807, Taiwan.

[4]Translational Research Center, Kaohsiung Medical University Hospital, 100 Tzyou 1st Road, Kaohsiung 807, Taiwan.

[5]Institute of Medical Science and Technology, National Sun Yat-Sen University, 70 Lienhai Road, Kaohsiung 804, Taiwan.

[6]Department of Electrical Engineering, College of Electrical Engineering & Computer Science, National Cheng Kung University, Tainan, Taiwan

[7]Institute of Chemistry, Academia Sinica, Taipei, Taiwan

[8] Institute of Biochemistry and Molecular Biology, National Yang-Ming University, Taipei, Taiwan

[9] Institute of Biomedical Chemistry RAMS, Moscow, Russia

Abstract

Tyrosine phosphorylation plays a critical role in cell biological functions, particularly in signal transduction. Mass spectrometry (MS)-based proteomic analysis of tyrosine-phosphorylated (pTyr) proteins remains challenging due to their relatively low abundance. The methods of phosphopeptide enrichment are developed prosperously such as IMmuno Affinity Chromatography (IMAC) and Metal Oxide Affinity Chromatography (MOAC). However, the complexity of experimental design for sample separation induces the unnecessary variations, particularly in label-free study designs. Here, we report an alternative approach, Inclusion List-driven Targeted LC-tandem MS (ILT LC-tandem MS), and demonstrate the results obtained are comparable with that of phosphopeptide enrichment for increasing the sequencing possibility of low abundant pTyr peptides. In the present study, ILT LC-M/MS was applied for comparative label-free quantitative tyrosine phosphor proteomic analysis between Src inhibitor (dasatinib)-treated and untreated CL1-5 lung cancer cells. A total of 512 distinct pTyr sites corresponding to 491 peptides had been identified.

According to evaluation using Mascot Delta score (MD-score), that 88.8% of the pTyr sites were considered confidently determined. In addition, the possibility of identifying multi phosphorylated peptides by ILT LC--tandem MS was 11% higher than that by TiO2-based phosphopeptide enrichment previously reported. After the comparative label-free quantitative analysis, among the 491 pTyr peptides identified 103 showed the significant level alteration of tyrosine phosphorylation between dasatinib-treated and untreated cells, and among which 53 altered pTyr peptides were matched to contain Src kinase substrate motifs. Using pathway analysis of the corresponding proteins, the results illustrated that 17 proteins were regulated by E2F transcription factor 1, which is known to be related to cell cycle regulation, and therefore provided a credible basis for further investigations. Our data demonstrate that the utility of an alternative approach, ILT LC--tandem MS, increases the sequencing possibility of low abundant pTyr peptides and reduces the induced variations in conventional TiO2 enrichment label-free quantitative analysis.

Keywords: Inclusion list-driven targeted LC--tandem MS; Label-free quantitative analysis; Tyrosine Phosphoproteomics; Phosphopeptide enrichment

***Corresponding Author:** Pao-Chi Liao, Department of Environmental Occupational Health, College of Medicine, National Cheng Kung University, 138 Sheng-Li Road, Tainan 70428, Taiwan; Tel: +886 6 2353535x5566; Fax: +886 6 2743748; E-mail: liaopc@mail.ncku.edu.tw

Introduction

Protein phosphorylation is a crucial protein post-translational modification that is involved in many biological processes, including signal transduction, cell cycle control, and differentiation [25]. In a typical eukaryotic cell, approximately 30%-50% of all proteins undergo some phosphorylation [43]. In eukaryotes, certain kinases catalyze the addition of a phosphate group to the side chains of hydroxyl-containing amino acids: Serine (Ser), Threonine (Thr) and Tyrosine (Tyr). Many human diseases (Eg: Cancer, diabetes, and Alzheimer's disease) are triggered by the dysregulation of phosphorylation and dephosphorylation [15, 41]. In particular, over 45 protein tyrosine kinases have been implicated in the pathogenesis of human cancers [5]. If the regulation of protein tyrosine phosphorylation is not properly controlled, normal cells may become malignant tumor cells, leading to carcinogenesis [40]. Tyrosine-phosphorylated (pTyr) proteins are currently among specific targets for the development of potential biomarkers for use in prognosis, diagnosis, and the prediction of drug responses, and some are considered to be promising drug targets [34]. Tyrosine phosphoproteomes, therefore, has attracted considerable attention in recent years [35].

Mass Spectrometry (MS)-based tyrosine phosphoproteomics is a comprehensive method for pTyr site determination and molecular signaling network elucidation [13, 56]. The process for identifying pTyr proteins remains to be improved due to the low abundance of targets (approximately 0.05% of the total human phosphoproteome consists of pTyr proteins), which presents a significant challenge for identification [39]. The primary technique used for pTyr protein enrichment is Immuno Precipitation (IP) using pTyr-specific antibodies [16, 46, 51]. Bergström Lind and co-workers used different combinations of antibodies, such as 4G10 and PY100, to create the optimal conditions for both pTyr protein and peptide level enrichment in the K562 leukemia cell line [3]. Their results indicated that protein identification following immuno affinity enrichment at the protein level gave greater sequence coverage than that at the peptide level. Subsequently, the Immobilized Metal Affinity Chromatography (IMAC) with Fe (III) or Ga (III), Metal Oxide Affinity Chromatography (MOAC) with TiO2 or ZrO2, or other materials, are often applied to increase the efficiency of phosphopeptide enrichment in conjunction with MS analysis [48, 6, 9, 26]. The underlying principle of these approaches is

that metal ions capture the negatively charged phosphoryl groups on the tryptic peptides form aqueous solution to achieve the effect phosphopeptide enrichment. While phosphoryl groups were captured, the non-phosphorylated peptides containing multiple acidic and/or histidine residues were also trapped and resulted in interference of the specificity of phosphopeptide enrichment [20]. To overcome the issues introduced from interference, various approaches were developed such as methyl esterification of carboxyl groups as derivatization agents [14] or addition of competitive additives into loading buffers [2, 31]. However, the subsequent derivatization procedure may induce side reactions and lead to introduction of artificial variations in subsequent MS-based analysis.

In our earliest work, we demonstrated a simple approach in which protein dephosphorylation with Alkaline Phosphatase (AP) provided a -80 (or multiple of -80) Da mass shift in the Matrix-Assisted Laser Desorption Ionization (MALDI)-based mass spectra [33]. This is a highly selective and sensitive method for determining the presence of phosphopeptides in numerous tryptic protein fragments. Following previous study, the enzymatic dephosphorylation coupled with a simple algorithm allowed possible phosphorylation signals to be distinguished within a large amount of LC-MS data after TiO2-based phosphopeptide enrichment [59]. In comparison with the typical LC--tandem MS analysis in data-dependent acquisition mode, the approach was carried out to lead to sequence more phosphor peptides in the casein peptide mixture. The recently developed hybrid linear trap (LTQ)/Orbitrap mass spectrometer [61], which was employed in a later study, had the advantages of high resolving power, rapid scan rate, and high mass accuracy, and enabled the more efficient and confident identification of protein phosphorylation sites. More recently, the approach has been applied to the label-free quantitative tyrosine phosphoproteome of human lung cancer cells to quantitatively identify the pTyr peptides involved in tumor metastasis [60]. However, the potential loss of low abundant pTyr peptides during phosphopeptide enrichment process prior to MS analysis is speculated.

To diminish the potential interference and loss of low abundant pTyr peptides, especially pTyr peptides, during enrichment prior MS analysis, we propose an alternative approach using the Inclusion List-driven Targeted LC--tandem MS (ILT LC-tandem MS), as depicted in Figure 1. With the samples in fewer processing steps of phosphopeptide enrichment prior MS analysis, the low abundant pTyr peptides may remain near complete conservation for LC-MS-based label free quantitative analysis. Meanwhile, the sample preparation procedures were kept as fewer as possible provides additional advantage to minimize the potential induced variations. Furthermore, a label-free quantitative tyrosine phosphoproteomic study using this alternative approach to comprehend the signaling pathway by Src kinase inhibitor (dasatinib)-treated highly invasive CL1-5 lung cancer cells is also reported herein.

Figure: 1

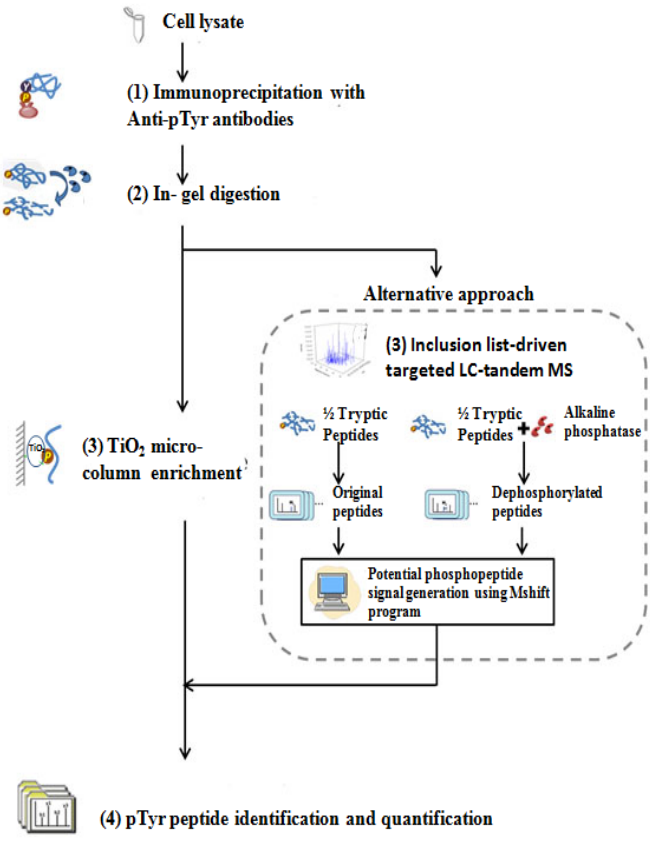

Figure 1: A schematic description of tradition and alternation of Inclusion List-driven Targeted (ILT) LC- tandem MS for the

tyrosine phosphopeptide enrichment, identification and quantification.

Material and Methods

Cell culture and Treatment

The CL1-5 cell line, which is a sub line of human lung adenocarcinoma cells selected by an in vitro invasion assay, was kindly provided by Dr. Pan-Chyr Yang (Academia Sinica, Taipei, Taiwan) [12]. CL1-5 cells were cultured in RPMI-1640 medium (Gibco, Gaithersburg, MD) supplemented with 10% fetal bovine serum (Gibco) and penicillin and streptomycin (Thermo Scientific, Logan, Utah) at 37°C containing 5% CO_2. Dasatinib (Santa Cruz Biotechnology, Santa Cruz, CA) was prepared at 0.1 mM in a DMSO vehicle (Sigma-Aldrich, St. Louis, MO) as the experimental storage dose. When the cultures achieved 70-80% confluence, the cells were treated with a final concentration of 0.1 μM dasatinib in a 0.1% DMSO vehicle for 48 h. The control (0.1% DMSO only) and dasatinib-treated CL1-5 cells were collected by centrifugation at 800 × g for 10 min. Both cell pellets were suspended in PBS containing phosphatase inhibitors (Roche Applied. Science, Indianapolis, IN) and subsequently disrupted by sonication time for 1 min at 20 W in 10-sec pulses on ice. After centrifuging at 12000 × g for 1 h, the supernatants were collected, some of which were then extracted, and the protein concentration was estimated by using Bicin Choninic Acid (BCA) protein assay (Pierce, Rockford, IL).

Immuno affinity enrichment of pTyr proteins

The 700 μg of extracted proteins were resuspended in 300 μl of Radio Immuno Precipitation Assay (RIPA) buffer (50 mM Tris-HCl, 150 mM NaCl, 1% NP-40, 0.5% sodium deoxycholate, 0.1% SDS) and reacted with 50 μl of agarose-immobilized pTyr-specific antibody 4G10 (Millipore, Temecula, CA) and PT-66 (Sigma-Aldrich) antibodies, as reported previously [60]. After interaction, the agarose beads were washed three times with 500 μl RIPA buffer and eluted using 40 μl 4× sample buffer (Invitrogen, La Jolla, CA) supplemented with 400 mM Di Thio Threitol (DTT). To concentrate the eluted proteins, an SDS-PAGE gel composed of a 5% acrylamide stacking gel and a 20% acrylamide separating gel was used [30, 11]. After electrophoresis at 50 V for 30 min, the proteins focused on the stacking gel and barely approached the separating gel. The gel was then stained with Coomassie blue for 1 h. The protein band was passed through a destaining solution and excised in pieces of 1 mm3, which were then subjected to in-gel digestion.

Tryptic in-gel digestion

The destained gel pieces were washed twice with a 1:1 solution of ACetoNitrile (ACN) and 25 mM ammonium bicarbonate. The protein mixtures were reduced and alkylated as previously described [60]. Trypsin digestion was performed at 37°C overnight, and the protein digests were dried completely.

TiO2 micro-columns enrichment of pTyr peptide

Prior to sample loading, the TiO2 micro-column was first rinsed with 100 μL of 80% ACN containing 2% Tri Fluoro Acetic acid (TFA). Subsequently, the TiO2 micro-column was equilibrated with loading buffer, 65% ACN and 2% TFA with saturated glutamic acid (J.T. Baker) for 2 min, repeated 3 times. The tryptic digested samples (30 μL) was diluted with 185 μL of loading buffer and loaded into TiO2 micro-column with a syringe pump set at a flow rate of 10 μL/min. The micro-column was washed in the following order: 20 μL of sample loading buffer, 20 μL of 65% ACN/0.5% TFA, and 20 μL of 65% ACN/0.1% TFA. To elute the bound peptides, Twice of 50 μL of 300 mM NH4OH/50% ACN were used. The eluted peptides were lyophilized for further MS analysis.

Enzymatic dephosphorylation

The control and dasatinib-treated samples were dissolved in dephosphorylation buffer (Roche) to adjust the pH value of the solution to 8, the optimal pH for Alkaline Phosphatase (AP) activity. A quarter of the dissolved sample was incubated with 0.25 U of AP (Roche) at 37°C for 2 h. Finally, the total four experimental groups of tryptic peptides of CL1-5, CL1-5 with

AP treatment, dasatinib-treated CL1-5, and dasatinib-treated CL1-5 with AP treatment were acidified with 2.5% TFA for peptide desalting (C18 pipet tips; Varian, Lake Forest, CA). The each group was performed in six replicates for the subsequent MS analysis.

NanoLC-MS analysis

The peptide mixtures were analyzed by full-scan LC-MS on a nanoAcquity system (Waters, Milford, MA) coupled to an LTQ-Orbitrap Velos hybrid mass spectrometer (Thermo Scientific) equipped with a PicoView nanospray interface (New Objective).

Peptide mixtures were loaded onto a 75-μm I.D. × 250-mm nanoACQUITY UPLC BEH130 column packed with diameter 1.7 μm particle of C18 resin (Waters) and separated at a flow rate of 200 nl/min using a linear gradient of 10% to 60% solvent B (80% acetonitrile with 0.1% formic acid) for 30 min, followed by a sharp increase to 100% B at 1 min and held at 100% B for another 10 min. Solvent A was 5% acetonitrile with 0.1% formic acid in water. The effluent from the HPLC column was directly electro sprayed into the mass spectrometer. The LTQ-Orbitrap Velos instrument was operated in full scan MS positive acquisition mode, and full scan MS spectra (m/z 300–2000) were acquired in the Orbitrap analyzer after accumulation to a target value of 1e6 in the linear ion trap. The resolution in the Orbitrap system was set to R = 60,000 (all Orbitrap system resolution values are given at m/z 400). The standard mass spectrometric conditions for all experiments were: spray voltage, 1.8 kV; no sheath and auxiliary gas flow; heated capillary temperature, 200°C; predictive Automatic Gain Control (AGC) enabled; and an S-lens RF level of 50%. The instrument was controlled by Tune 2.6.0 and X calibur

Software

Generation of inclusion list of phosphopeptide signal candidates

The raw files generated by the LTQ-Orbitrap Velos hybrid mass spectrometer were converted to the open file representation format mzXML using the ReAdW program developed by the Seattle Proteome Center (SPC). The open-source ReAdW software was downloaded from http://tools.proteomecenter.org/software.php/. Another open-source program, msInspect, which was developed by the Computational Proteomics Laboratory (CPL), was used to process the operational analysis to acquire peak information after peak detection, mono isotopic peak determination, and the calculation of original masses. The ms Inspect program is available at http://proteomics.fhcrc.org/. An in-house program, MShift, used the peak information from ms Inspect processing to find the potential phosphopeptide signals according to a mass shift of -79.966 (or multiple of -79.966) Da upon dephosphorylation. MShift program is designed so that users can customize the m/z by inputting the parameters to generate an inclusion list of phosphopeptide signal candidates for targeted LC--tandem MS analysis.

Targeted LC--tandem MS analysis and Database search

The m/z values of possible phosphopeptide signals obtained from MShift program process were set in the parent mass list on an ion trap mass spectrometer (LCQ DECA XP Plus, Thermo Finnigan), which triggered tandem MS analysis once these m/z values were observed. Each cycle contained one full scan mass spectrum (m/z 300–2000) followed by three tandem mass spectra with the collision energy set at 35%. Bio works Browser 3.1 (Thermo Scientific) was used to transform all tandem MS files from Thermo raw to the DTA file format. A Perl script, merge.pl, was used to concatenate the generated DTA files on the Matrix Science Web site (http://www.apcf.edu.au/mascot/help/instruments_xcalibur.html). The tandem MS peak list was submitted to an in-house Mascot server (Version: 2.2, Matrix Science Ltd., London, UK) for search against the Swiss-Prot human non-redundant database (Database: SwissProt 090616 (468851 sequences); Taxonomy: Homo sapiens (20401 sequences)) with a confidence level of 95% or greater. Up to two missed cleavages were allowed for the trypsin-specific performance. Carboxy amido methylation on Cys, deamidation on Asp and Glu, oxidation on Met, and

phosphorylation on Ser, Thr, and Tyr were allowed as variable modifications. Mass deviations for precursor ions and fragment ions were all set to 1 Da. A false discovery rate of ≤ 5% was calculated by the Mascot-integrated decoy database search. Finally, the following three criteria were used to assess the results: (1) the Mascot search result reported pTyr modification, (2) the pTyr peptide score was above 25, (3) the pTyr peptide was the rank 1 in the same tandem MS spectrum, and (4) more than three b or y ions adjacent to or on the assigned pTyr site were manually confirmed by visual assessment of the tandem MS data. Only results that met all of these criteria were identified as approved pTyr peptides in this study.

Relative label-free quantitation of identified pTyr peptides

Peak lists of LC-MS runs were aligned by Progenesis LC-MS software (Nonlinear Dynamics, Newcastle upon Tyne, UK). One run was chosen as the alignment reference and the other runs were automatically aligned to the reference according to their retention times. Each run was illustrated by a proprietary algorithm as a two-dimensional feature map as m/z values versus Retention Time (RT). Features with fewer than three isotopes and only one charge were masked at this point and excluded from further analyses. The control and treated runs were then divided into two appropriate groups and the raw abundances (areas under the peaks) of all features were normalized. A quantitative abundance ratio of each feature was calculated automatically between the normalization run and the reference run. After Normalization, One-way Analysis of Variance (ANOVA) was performed on all features in all sample runs using transformed normalized abundances. The features with charges < +2 charge were masked and excluded from further analyses, and all remaining features were used to calculate a normalization factor to correct the experimental variation between runs. After normalization, a statistical analysis was performed by using transformed “loglike” arcsine (ANOVA) calculations of all the detected features. The MShift program added an extra function, which utilized the parameters of m/z values, RT adjustment, and charge state, link up with the qualitative identification and quantitative proteomics analysis in a tyrosine phosphoproteomic research. These aligned results were manually reconfirmed by patterns of peaks in close proximity. To relatively quantify pTyr peptide levels, the ANOVA values with $p \leq 0.01$ were regarded as significantly altered pTyr peptides between control and dasatinib-treated groups.

Bioinformatics Analysis

For the confident localization of identified pTyr site, the tool of Mascot Delta Score (MD-score) calculated the difference Mascot scores between the top two alternative phosphorylation sites in same peptide sequence [49]. The MD-score more than 5 is an evaluative threshold of confident phosphopeptide site identification [52, 57]. We used this condition to analyze the all identified pTyr peptides. A tool, Phospho RS, in the Proteome Discoverer (version 1.3, Thermo. Scientific) enabled to provide the individual probability values for each putatively phosphorylated site based on the given tandem MS data [53]. According to the reference, the cut-off value was set as 70% of phospho RS site probability to lead to an acceptable false localization rate. The Motif Matcher in phosphorylation site database (PHOSIDA; http://www.phosida.com) was applied to predict the potential pTyr sites [18]. The extended seven residues before and after the identified pTyr sites were submitted to the textbox of Motif Matcher. The sequence search in Phospho Site Plus (PSP; http://www.phosphosite.org/homeAction.do) was also used to analyze the identified peptides that that contain pTyr sites within them [24]. In addition, the pTyr sites were categorized to belong to what kind of tyrosine kinase/phosphatase substrate motifs using Phospho Motif Finder in Human Protein Reference Database (http://www.hprd.org/PhosphoMotif_finder) [1]. After Phospho Motif Finder analysis, the accession numbers of Src-associated pTyr peptides were uploaded and analyzed for evidence of a protein-protein interaction network using an integrated knowledge and software suite, Meta Core TM (Gene Go, Inc., St. Joseph, MI).

Results and Discussion

Determination of dasatinib (Sprycel®) treatment concentration on CL1-5 lung cancer cells

To further understand the Src-mediated tyrosine phosphorylation using the treatment of Src inhibitor, dasatinib (Sprycel®), a series of experiments were design using highly invasive CL1-5 cells, initiated by earlier study of the altered pTyr proteins involved in the signaling pathway by Src in lung cancer metastasis. The CL1-5 cells with and without dasatinib (Sprycel®) treatment were regarded as the treatment and control groups. Dasatinib (Sprycel®) is an anti-cancer drug that possess inhibit Src family tyrosine kinases activity, and it is, therefore, frequently used in experiments to evaluate the fold changes of Src-mediated proteins before and after treatment for an in-depth insight into the interactive relationship between drug and targets [19, 37]. To determine optimal dasatinib (Sprycel®) treatment concentration, the CL1-5 cells were treated with different concentrations (0, 0.001, 0.01, 0.1, 1, and 10 μM, respectively) of dasatinib (Sprycel®) using MTT assay, wound healing assay, Transwell assay, and Matrigel assay followed by subsequent comparative tyrosine phosphoproteomic approach. The selection principle was dependent on the minimum effects on cell viability, but the cell migration and invasive abilities of CL1-5 cells were significantly decreased. The results indicated that treatment with 0.1 μM dasatinib on CL1-5 cells maintained the cell survival rate at 102±3%. Nevertheless, the cell migration and invasion decreased to 40% and 58% ($p<0.05$). For the comparative study, the treatment group was performed in the presence of dasatinib at the concentration of 0.1 μM on CL1-5 cells. This same concentration corresponded to other cell lines reported from different literatures [8, 7, 44].

Workflow design of the experiment

As shown in the workflow of Figure.1, prior to MS analysis, in order to diminish the potential interference and increasing the signals of phospho tyrosine protein and reducing the signals of non-phospho proteins interference, the extracting proteins from the CL1-5 cells with and without dasatinib (Sprycel®) as control group and reacted with anti-pTyr antibodies 4G10 and PT66. The preliminary prepared samples from immuno precipitation enrichment were subjected stacking-gel for protein concentration and in-gel tryptic digestion. After trypsin digestion, the sample of digested peptides was aliquot into two portions. The first portion was further enriched by TiO2 micro-column enrichment in order to reduce non-phosphopeptides after trypsin digestion and then the eluted sample was analyzed by LC-tandem MS. The other portion from in-gel digestion was alternative further treated or untreated with AP. These two samples of treated or untreated with AP were assayed with LC-MS. The alternative approach of ILT LC-tandem MS, a comparative analysis of LC-MS signals from treated or untreated with AP by home- developed MShift software to produce the inclusion list of possible phosphopeptide signal candidates and for further targeted LC-tandem MS analysis.

LC- tandem MS analysis for further TiO2 micro-column enrichment and Mascot database search

The tandem MS data of the peptides enriched from TiO2 micro-column enrichment after in-gel trypsin digestion and immuno affinity purification lung cancer CL1-5 cell extract was analyzed by an in-house Mascot server (Version: 2.2, Matrix Science Ltd., London, UK) for search against the Swiss-Prot human non-redundant database; Taxonomy: Homo sapiens with a confidence level of 95% or greater. Up to two missed cleavages were allowed for the trypsin-specific performance. Carboxy amido methylation on cysteine, deamidation on aspartic acid and glutamic acid, oxidation on methionine, and phosphorylation on serine, Threonine, and tyrosine were allowed as variable modifications. Mass deviations for precursor ions and fragment ions were all set to 1 Da. A false discovery rate of ≤ 5% was calculated by the Mascot-integrated decoy database search. MASCOT generic file was searched for peptide identification. Total numbers of identified peptides were 3397 (supplementary Table 1) from replicate LC- tandem MS datasets. The modifications of phosphorylation peptides including tyrosine-, serine-, and Threonine were reported for 407 phosphopeptides; however there only 5 tyrosine phospeptides were identified (supplementary Table 2) which

were peptide score was above 20, and the peptide is blot was the 1. The phosphopeptide selectivity from further TiO2 micro-column enrichment after in-gel trypsin digested and immuno affinity enrichment lung cancer CL1-5 cell extract was 12% (406/3397). The numbers of tyrosine phosphopeptides were only 1% (5/407) of total identified phosphopeptides.

The Inclusion list of possible phosphopeptides from MShift program analysis and targeted LC- tandem M

The MShift program was applied to each LC-MS run (six replicated analyses of each of four samples: (1) CL1-5 cell lysate untreated with AP, (2) CL1-5 lysate treated with AP, (3) dasatinib-treated CL1-5 lysate untreated with AP, and (4) dasatinib-treated CL1-5 treated with AP. . It could simultaneously perform data analysis for the control or treatment group of six replicate LC-MS datasets with versus without AP treatment to increase the efficiency of phosphopeptide signals mining. The same functional program, Delta Finder, we developed previously to process only one pair of LC-MS datasets. Figure 2 illustrated the MShift program based on the algorithm to generate an m/z value of phosphopeptide signal candidate. The computing algorithm of MShift program utilized the mono isotopic peak information from the LC-MS datasets with and without AP treatment to calculate the peak pairs with a mass shift corresponding to phosphate group(s) loss ($nHPO_3$: -79.966n Da). In a given peak pair, one value from the dataset without AP treatment was as a phosphopeptide signal candidate triggering an tandem MS acquisition as shown in Figure 2. After processing, the original peptide mass of 1133.5366 Da (from m/z 378.852, 3+) in the untreated run compared with 1053.5577 Da (from m/z 527.786, 2+) in the de phosphorylated run for a difference of -79.9789 Da. The m/z of 378.852 was rounded to 378.9 as the possible peak signal for the inclusion list of phosphopeptide candidates trigging the tandem MS acquisition. On the other side, we applied a label-free LC-MS quantitative tool, Progenesis LC-MS, to obtain a peak quantitative result due to the landmark-driven peaks alignment and its ion intensities. Finally, we developed MShift program to connect the results of qualitative identification and quantitative analysis via m/z, charge state, and retention time for label-free quantitative tyrosine phosphoproteomics.

Figure: 2

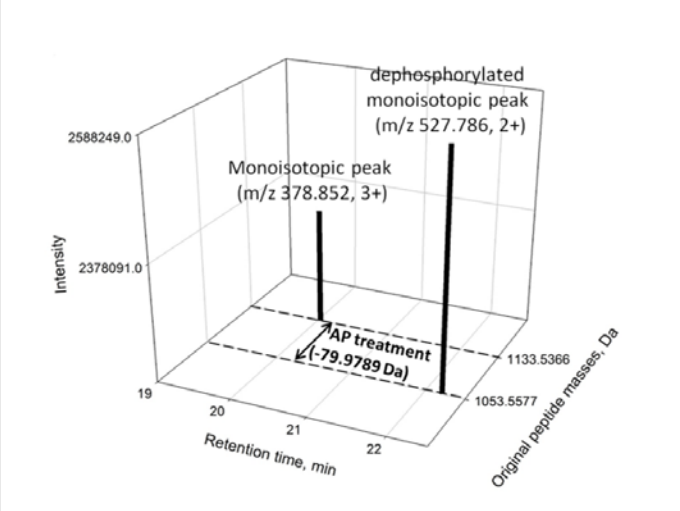

Figure 2: Three-dimensional representations of one phosphopeptide signal candidate in the inclusion before and after enzymatic dephosphorylation. According to the signal from mass shift calculation, a mono isotopic peak (m/z 378.852, 3+; original mass 1133.5366 Da) was chosen for targeted LC-tandem MS analysis and illustrated as a three dimensional representation. After dephosphorylation, the original mass from 1133.5366 Da shifted to 1053.5577 Da and the difference of 79.9789 Da was a phosphate group (HPO_3) loss. The peak retention time also shifted from 20 min to 22.2 min. This selected peak within the inclusion list was subjected to tandem MS acquisition and therefore the product ion spectrum illustrated in Figure 4A.

In recent years, similar approaches were developed. Jaffe and co-workers presented a new technology, accurate inclusion mass screening (AIMS), that the identification efficiency of an interesting peptide increased at least 4-fold as compare with undirected LC- tandem MS experiments in the same instrument [27]. Schmidt and co-workers also demonstrated that the inclusion list-based method had higher specificity and reproducibility of identified peptides in the same sample than standard data dependent acquisition method, specifically in low

intensity precursor ions [50]. Although the distinct difference of the generation strategies of inclusion list described above (including our approach), the applications allowed to sequence the low abundance peptides in complex mixtures and further increase overall proteome coverage. In addition to ILT LC-tandem MS, the samples of label-free quantitative LC-MS datasets without phosphopeptide enrichment processing could hold the true peak intensities without distortion due to the reduction of variations by using as fewer as possible experiments. In this study, the combination of pattern-based quantitative method and targeted LC-tandem MS overcame the poor reproducibility of low abundance phosphopeptides, especially pTyr peptides, because the data-dependent acquisition mode favored to sequence the peptides of highest abundance that represent only a fraction of the detectable m/z peaks in LC-tandem MS based quantitative method.

Identification of pTyr Peptides

According to the depiction of Figure 2, 3 illustrated how to generate an inclusion list of phosphopeptide signal candidates in high-throughput LC-MS analyses. Approximately 30,000 mono isotopic peaks were present in each of the 24 LC-MS datasets after processing. The 81-87% mono isotopic peaks were overlapped across each sample of six replicate LC-MS datasets due to the parameters: m/z tolerance of 0.02 Da and retention time tolerance of 30 sec. This result indicated that the six replicate LC-MS datasets in each sample had good peak reproducibility. Therefore, we chose two LC-MS datasets from CL1-5 and CL1-5 with AP treatment respectively to display how to filter out the large non-related peak signals as shown in Figure 3A and 3B. If the peak signals were enormously complex to lead to increase the chance of random match of mass differences (-79.966n Da, n=1, 2, 3…) between the control or treatment group with and without AP treatment, it was difficult to pick the correct phosphopeptide signals. To avoid the interference of noise, the appropriate cut-off values lets user set the value based on the analytic data of distribution of peak intensity versus peak numbers using MShift program. In this study, the cut-off values were set at 2,000. In addition, according to the computing algorithm as $\square\Delta - 79.966n \mid \leq \kappa$ (Δ is mass shift calculation, n is the number of phosphate groups, and κ is maximum mass shift tolerance), the parameters were set that κ was 0.05 Da, n was less than 5, and retention time tolerance after dephosphorylation was within 5 min. These parameters were set based on the literature and our previous work [36, 61]. Finally, 419 m/z values were generated after redundant m/z value deletion (Figure 3C). The significantly lower peak intensities of 419 m/z values in Figure 3C compared to that of Figure 3A and B indicated that our approach can extract the low abundance phosphopeptide signals, which may be not performed by the tandem MS acquisition in data-dependent mode, into the inclusion list to increase the probability and reproducibility of identification, particularly in pTyr peptides.

Figure: 3

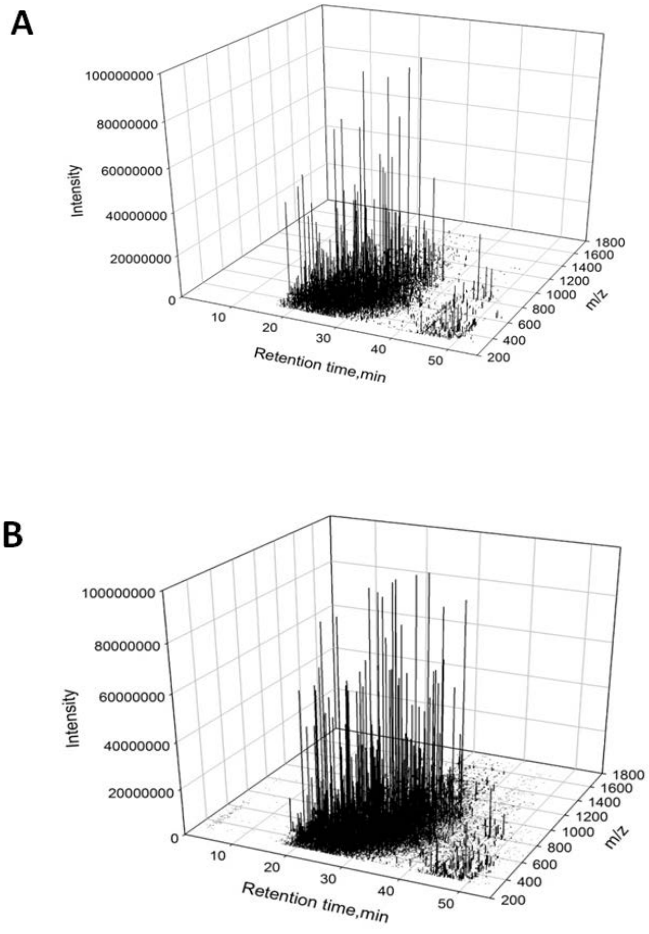

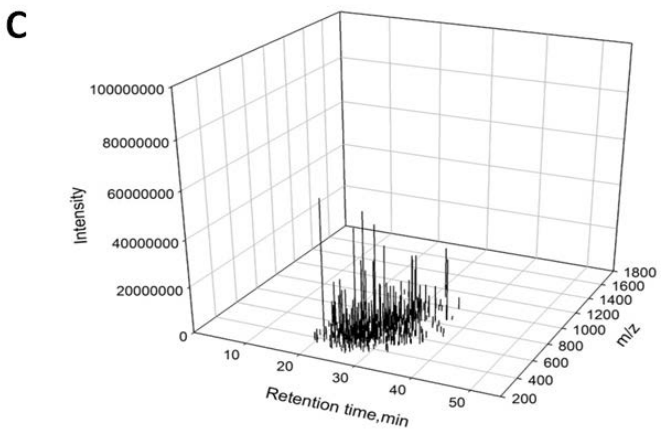

Figure 3: An illustrated depiction of the inclusion list of 419 phosphopeptide signal candidates from large scale LC-MS experiments with and without Alkaline Phosphatase (AP) treatment. (A) The use of one LC-MS dataset of six replicates without AP-treated CL1-5 cells was diagramed according to the retention time (X-axis), m/z (Y-axis), and intensity (Z-axis). There are 27,897 mono isotopic peak signals after de isotope. (B) The 33,310 mono isotopic peak signals were from one LC-MS dataset with AP treatment. (C) The 419 possible phosphopeptide signals with a mass shift corresponding to phosphate (HPO_3) group(s) loss that were picked by the in-house program, MShift.

After LC-MS analyses, the residual samples of tryptic peptides pooled from control and treatment groups were then subjected to LCQ mass spectrometer for targeted LC- tandem MS analyses with this set of values provided as the parent mass list. Due to an intrinsic limitation of the LCQ mass spectrometer, which is that only 25 m/z values can be imported into the parent mass list for each targeted LC- tandem MS run, the total 17 runs were performed to achieve most of the identification. Finally, A total of 491 pTyr peptides containing 512 pTyr sites were identified from 242 (58%) of the 419 parent m/z values. Because the setting of parent masses in LCQ was not divided into segments by retention time, each m/z value may match more than one pTyr peptide with a different retention time. After calculation of the distribution of pTyr peptides among all identified phosphopeptides, the result indicated that the alternative approach increased the chance of pTyr peptide identification from 0.05% theoretical probability [39] to 8.7%. The probability of 8.7% pTyr peptide identification still resembled the 9.3% in our previous approach with additional TiO2-based phosphopeptide enrichment [60]. Subsequently, the targeted LC-tandem MS analyses could obtain the high-quality tandem MS spectra to assign confidence of pTyr sites determination within the phosphopeptides. For example, as shown in Figure 4A, the pTyr peptide sequence (EDoxiMPIDpYR) of geminin coiled-coil domain-containing protein 1 was identified by the Mascot search engine. The parent mass of the tandem MS spectrum was m/z 378.9 with a charge state of 3+ as depicted in Figure 2. The b62+ and y22+ ions make unambiguously the phosphorylation site determination on Y245. In Fig. 4B, the sequence of RINHpSSDQGISSpYpTKLK belongs to sacsin with charge state 3 at m/z 725.40. The fragment ions of [y13-196]3+, [y12-98]2+, [y5-98] +, [y4-98] + and y3+ ions suggested the multi phosphorylation sites on S933, Y941 and T942. In Figure 4C, the identified pTyr peptide (HpSKPTpSAYpYpTR) belongs to leucine-rich repeat flightless-interacting protein 2 with charge state 3 at m/z 544.30. The S162, S166, Y169, and T170 were phosphorylated due to the [y10-294]2+, [y9-196]2+, [y6-196]2+, [y5-98]+, [y3-98-NH3]2+ and y1+ ions. The neutral losses of H3PO4, 2H3PO4, and 3H3PO4 are -98, -196 and -294 Da. Therefore, the results demonstrated that ILT LC- tandem MS enabled to improve the quality of the tandem MS spectra for the pTyr peptides.

Figure: 4

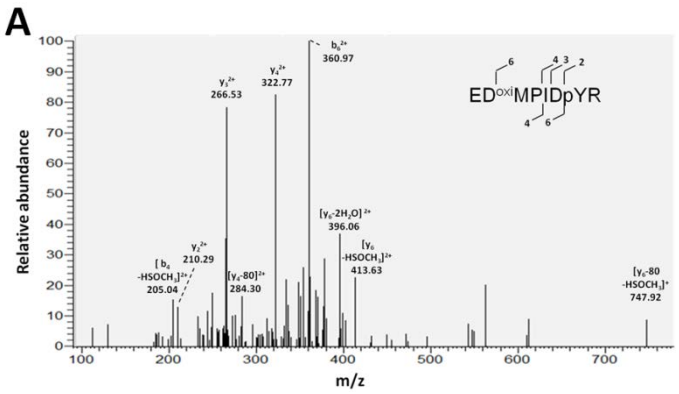

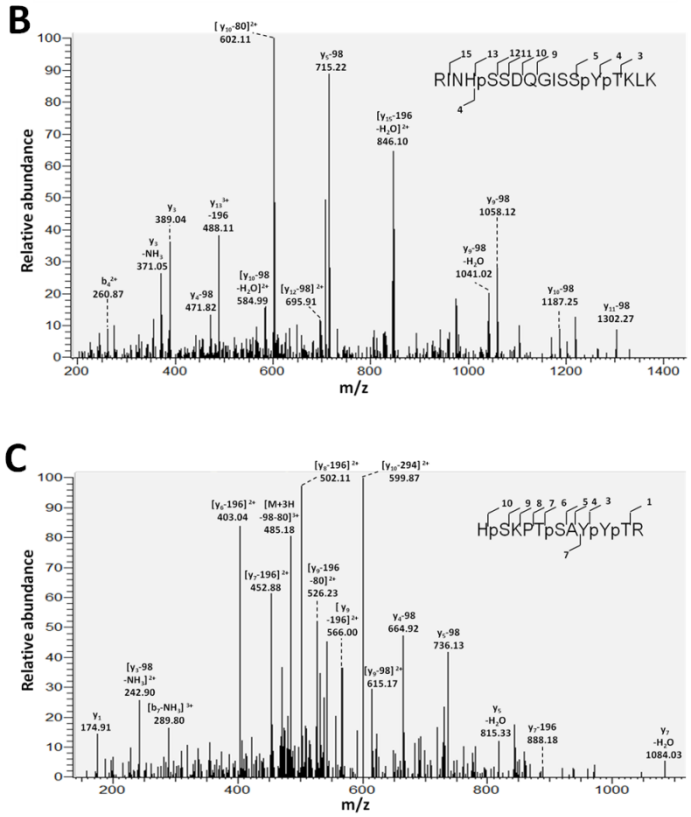

Figure 4: Tandem MS spectra of three identified pTyr peptides. (A) The tandem MS spectrum result showed that the identified pTyr peptide (EDoxiMPIDpYR) belongs to geminin coiled-coil domain-containing protein 1 (m/z 378.9, 3+). (B) The identified pTyr peptide (RINHpSSDQGISSpYpTKLK) belongs to sacsin (m/z 725.40, 3+). (C) The identified pTyr peptide (HpSKPTpSAYpYpTR) belongs to leucine-rich repeat flightless-interacting protein 2 (m/z 544.30, 3+). The b and y ions were manually inspected and annotated.

Evaluation of the pTyr peptide identification and quantification

Mascot Delta score (MD-score) is a robust tool to estimate the probability of correct phosphorylation site localization. The role of MD-score is to measure the difference between the top two Mascot ion scores of alternative phosphorylation site localizations in same peptide sequence. Savitski and co-workers remarked that MD-score exceeded Ascore in determination of pTyr site accuracy [49]. If the MD-score was more than 5, the top-ranked pTyr site is considered confidently determined [32]. Here we compared the distribution of MD-score of 491 identified pTyr peptides with the previous identification of 276 pTyr peptides from the workflow with TiO2-based phosphopeptide enrichment at Wu et al., 2010 (Figure 5A). In present result, up to 88.8% of pTyr peptides, including the examples in Figure 4, were MD-score > 5 even higher than 82% in the previous identification. In the other tool, phospho RS, was also used to evaluate confident pTyr site localization. If phospho RS site probability cutoff was more than 70%, the identified pTyr sites is considered the low false localization rate [53]. The present and previous results were 43.5% and 47.4% respectively to over 70% of phospho RS site probability (Figure 5B). The result demonstrated that the ILT LC-tandem MS enabled to make up the function of TiO2-based phosphopeptide enrichment. In addition, 170 (33.2%) identified pTyr sites corresponding to 163 pTyr peptides were matched to contain the conserved tyrosine kinase motifs using Motif Matcher program in phosphorylation site database (PHOSIDA) (Figure 5C) [17]. In previous result, 30.4% pTyr sites were matched. The other tool, Phospho Site Plus (PSP), was used to evaluate the identified peptides that contain pTyr sites within them. The result indicated the 19.5% and 22.1% identified pTyr sites against PSP in present and previous result (Figure 5D). It meant that the alternative approach still determined the confident pTyr site to be phosphorylated by known tyrosine kinases. The cellular locations and molecular functions of 491 pTyr peptides were analyzed using Gene Ontology database. The distribution was similar to previous result that most proteins were still found to be located in the membrane (19%) and involved in protein binding interaction (21%). In addition, all 512 pTyr sites, which expended in both forward and backward seven residues, were submitted to Phospho Motif Finder program, which is available from the Human Protein Reference Database at http://www.hprd.org/PhosphoMotif_finder/ [1, 29]. The 28.3% pTyr sites were categorized to Src kinase substrate motif of pY [A/G/S/T/E/D]. Furthermore, the present workflow without TiO2-based phosphopeptide enrichment could increase the possibility of identifying multi phosphorylated peptides, because TiO2 possessed too strong binding force with multiple

phosphate groups in a peptide to be eluted. After analysis of the ratio of multi phosphorylated peptides among all phosphopeptides, the ratio in the present workflow was 11% more than in the previous workflow with additional procedure of TiO2-based phosphopeptide enrichment. These evaluations supported that the ILT LC- tandem MS provided the confident pTyr site determination, even reduced the loss of multi phosphorylated peptides.

The two groups of six replicate LC-MS datasets from control (CL1-5 cells) and treatment (dasatinib-treated CL1-5 cells) without AP treatment were aligned by Progenesis LC-MS software. After normalization, a total of 32,212 features were generated from the alignment of these two groups based on the drift of retention time in each LC-MS run compared to the reference run. Among the 491 pTyr peptides identified, 474 were quantified by the fold change of tyrosine-phosphorylated expression level between control and treatment groups within 12 runs of each feature according to the normalized ion abundance measurement in Progenesis LC-MS output data. Subsequently, MShift program based on the information of m/z values, RT, and charge state to link up with the identification of pTyr peptides from targeted LC- tandem MS analyses and the quantification of peak features from pattern-based quantitative method. The results of quantitative pTyr peptide were manually inspected and wound excluded once incorrectly aligned. The normalized dasatinib-treated/control ratios ranged from ~2-5 to ~22, were log2-transformed to account for the ratio metric data, and diagrammed as a value-order plot and histogram (Figure 5E and 5F). Because the majority of pTyr peptides tend to have similar abundances in control and treatment groups, the experimental distribution was fitted to a normal distribution based on the central limit theorem. To examine the significance of pTyr peptide levels between control and treatment groups using ANOVA test, a significance level of less than 0.01 was accepted. A total of 103 pTyr peptides had significant differences in expression with 36 and 67 pTyr peptides with higher expression levels in control and dasatinib-treated CL1-5 cells, respectively.

Figure: 5

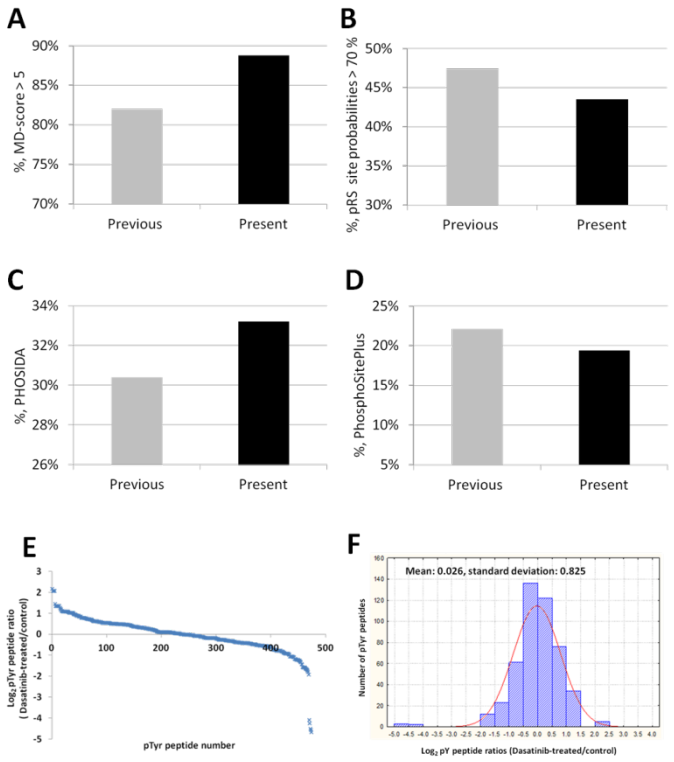

Figure 5: The evaluation of characterization of the pTyr peptide identification and quantification. (A) The confidence of pTyr site localization was estimated by a simple method, Mascot Delta Score (MD-score; Savitski et al., 2011), to compare the possibility of MD-score > 5 in the present identified pTyr sites with the previous without TiO2-based phosphopeptide enrichment (Wu et al., 2010). The bar chart showed that the percentage of 88.8% and 82% identified pTyr sites were MD-score > 5 from the present and previous results. (B) The phosphoRS were applied to evaluate the efficient and reliable localization of pTyr sites in peptides. The bar chart showed that the percentage of 43.5% and 47.4% identified pTyr sites were phospho RS site probability > 70% from the present and previous results. (C) The prediction of tyrosine kinase motifs was performed by a tool, Motif Matcher program in phosphorylation site database (PHOSIDA). The bar chart showed that the percentage of 33.2% and 30.4% identified pTyr sites, which expended seven residues in N-terminal and C-terminal to be subjected to Motif Matcher, corresponded to tyrosine kinase motifs. (D) The tool, Phospho Site Plus,

identified and displayed the sequences that contain pTyr sites with them. The bar chart showed that the percentage of 19.4% and 22.1% identified pTyr sites were considered confidently determined. (E) Distribution of the distinct expression level of tyrosine phosphorylation in control and dasatinib-treated CL1-5 cells was diagramed. The value-order plot of log2 ratio distribution reveals the fold-change of altered pTyr proteins. (F) Histogram shows that the number of pTyr peptides binned with a range from -5 to 4 according to log2 ratios. Values for the means and standard deviations were obtained by Gaussian regression analysis. The red line and the blue bars represent the normal and experimental distributions, respectively.

Characterization of the altered pTyr Peptides

For motif analysis, we used Phospho Motif Finder program to analyze the 105 pTyr sites within 103 altered pTyr peptides to obtain the distribution of tyrosine kinase and phosphatase substrate motifs (Figure 6A). Consequently, a total of 157 features of tyrosine kinase substrate motifs were identified. The 53 (51.5%) Src kinase substrate motifs were the main group among 103 altered pTyr peptides. After comparison of the ratio of Src kinase substrate motifs, the ratio increased from 28.3% of 512 identified pTyr sites to 51.5% of 105 altered pTyr sites. The treatment of dasatinib was a Src kinase inhibitor in CL1-5 cells, and found that the significant change of tyrosine phosphorylation level in associated proteins was identical with expectation. Therefore, the cell abilities of migration and invasion were influenced significantly. To confirm the significance of the altered pTyr peptides found in this investigation, we performed a pathway analysis using MetaCore software (GeneGo, Inc.). As shown in Figure 6B and Table 1, up to 17 proteins among the 53 altered pTyr peptides with Src kinase substrate motifs were regulated by the E2F transcription Factor 1 (E2F1). E2F1 plays a crucial role in apoptosis and cell cycle regulation, as demonstrated in a variety of experiments [21, 42]. According to an E2F1 binding site within the promoter, the E2F1 bound DNA and regulated gene transcription of 17 proteins in the pathway [4, 10, 28, 38]. The results of this work, which applied the ILT LC- tandem MS to the analysis of low abundant pTyr peptides, suggested that the relationship between dasatinib, the altered Src-associated pTyr proteins, and E2F1 may be a fruitful subject for further research in metastatic lung cancer.

Figure: 6

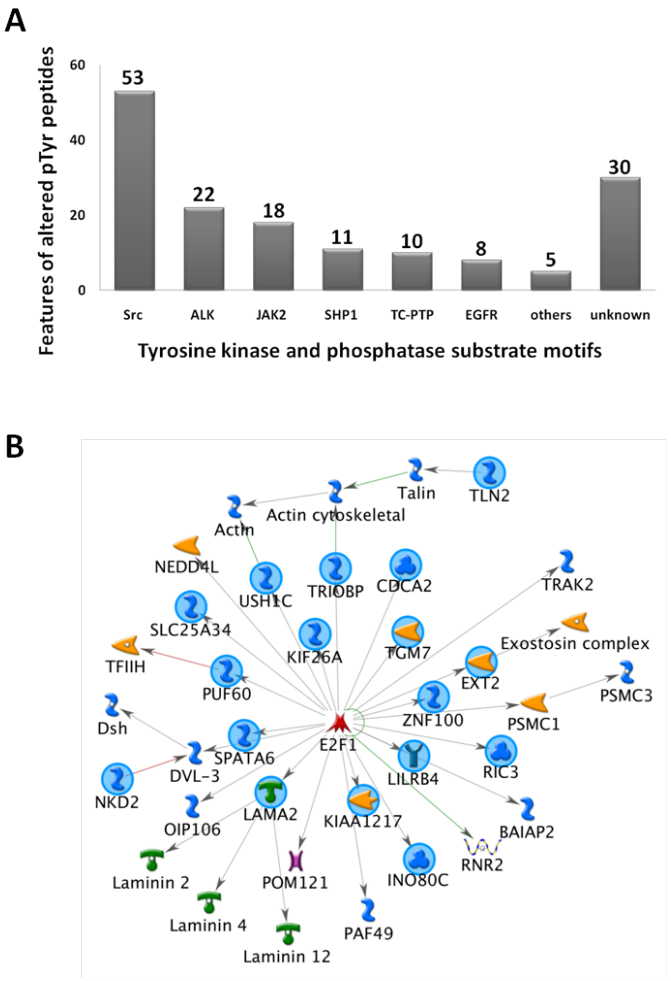

Figure 6: Investigation of the relationships among the altered pTyr proteins. (A) The distribution of tyrosine kinase/phosphatase substrate motifs in the altered pTyr peptides using the Phospho Motif Finder search tool from the Human Protein Reference Database. (B) Interaction network analysis of the corresponding proteins against the altered pTyr peptides with Src substrate motifs using MetaCore software implicated regulation by E2F transcription factor 1 (E2F1). The corresponding proteins in this study are marked with blue circles and are listed in Table 1. The symbols and links shown

on the network illustration include: generic binding protein ( ), generic receptor ( ), generic channel ( ), generic enzyme ( ), protein kinase ( ), protein phosphatase ( ), transcription factor ( ), protein ( ), activation ( ), inhibition ( ), and unspecified ( ).

In further discussion, only four proteins (LILRB4, TRIOBP, KIAA1217, and TLN2) in Figure 6B had been reported to be phosphorylated the tyrosine residues by kinase, but not in-depth investigation of their functional mechanisms by tyrosine phosphorylation [22, 45, 58]. This result revealed that the low abundant pTyr peptides were considerably added to the difficulty of comprehensive identification. In the interaction network, CDCA2 and USH1C were reported to relate to cell cycle regulation [23, 54]. CDCA2, alternative name Repo-Man, cooperated with protein phosphatase 1 and condensin to protect chromosome architecture to segregate at anaphase onset [55]. In the present study, the tyrosine-phosphorylated level of CDCA2 was up regulated in dasatinib-treated CL1-5 cells (1.24 fold), which suggested that the tyrosine phosphorylation expression might affect CDCA2 to regulate the mitotic chromosome structure. To the best of my knowledge, CDCA2 was described the up regulation of activator of cell cycle progression in melanoma cells, not in lung cancer cells. Besides, USH1C has the similar function to interact with the catalytic subunit of protein phosphatase 2A and cause G2/M cell cycle arrest in colon cancer cells [47]. The higher expression level of tyrosine phosphorylation of USH1C in dasatinib treatment was 1.45 fold as similar as the tendency of CDCA2. The relative investigations were still in the beginning and therefore our results might provide other research interests.

Table 1: Seventeen altered pTyr peptides with a Src kinase substrate motif in the extracted interaction network

no.	SwissProt no.	Gene name	Protein name	Sequence	Ratio (dasatinib-treated/ control)
01	Q8NHJ6	LILRB4	Leukocyte immunoglobulin-like receptor subfamily B member 4	NKARFSIPSMTEDpYAGR	2.55
02	Q96PF1	TGM7	Protein-glutamine gamma-glutamyltransferase Z	pYGQCWVFASVMCpTVMR	2.04
03	Q6PIV7	SLC25A34	Solute carrier family 25 member 34	GQLpYGGLTDCMVK	2.00
04	Q8IYN0	ZNF100	Zinc finger protein 100	pYGKpYGHDNLQLQK	1.84
05	Q9H2D6	TRIOBP	TRIO and F-actin-binding protein	ENALHSpYSTQKGPLK	1.62
06	Q9NWH7	SPATA6	Spermatogenesis-associated protein 6	NYEQPTIpSSKSHSPSPpYTK	1.54
07	P24043	LAMA2	Laminin subunit alpha-2	CARGpYpTGpYPDCKACNCSGLGSK	1.53
08	Q5T5P2	KIAA1217	Sickle tail protein homolog	IPpYGGTRSMVVPGNATIPR	1.50

09	Q9Y4G6	TLN2	Talin-2	pYpSKAIAVTAQEMMTK	1.46
10	Q9Y6N9	USH1C	Harmonin	HQVEpYDQLpTPR	1.45
11	Q969F2	NKD2	Protein naked cuticle homolog 2	EpSPEGDSFVASApYASGR	1.40
12	Q9ULI4	KIF26A	Kinesin-like protein KIF26A	pYASSpSSGGESSCEEGR	1.37
13	Q69YH5	CDCA2	Cell division cycle-associated protein 2	pYDVpSEFCSpYIK	1.24
14	Q6PI98	INO80C	INO80 complex subunit C	RPASPpSHNGSSGGGpYGApSKKK	0.77
15	Q93063	EXT2	Exostosin-2	MSDVpYpSILQSIPQR	0.75
16	Q9UHX1	PUF60	Poly(U)-binding-splicing factor PUF60	KpYAMEQSIKpSVLVK	0.75
17	Q7Z5B4	RIC3	Protein RIC-3	CpYpTAMPGNpTHRK	0.28

Conclusion

In this study, we described an alternative approach using Inclusion List-driven Targeted LC-tandem MS (ILT LC-tandem MS) that allowed the identification of the pTyr sites without phosphopeptide enrichment step and its application in comparative label-free quantitative method. According to dephosphorylation and mass shift calculation, the inclusion list of phosphopeptide signal candidates was generated to increase the accuracy of phosphopeptide identification, especially for rare pTyr peptides. The purpose was similar to that of phosphopeptide enrichment which selected the phosphorylated peptides (or their signals) for increasing the sequencing possibility in LC-tandem MS acquisition. In addition, the alternative approach could potentially avoid the loss of identifying multi phosphorylated peptides due to the interference of TiO2 strong binding force. Moreover, we developed an in-house program, MShift, designed to simultaneously process the multiple LC-MS datasets with and without AP treatment and generate the inclusion list of phosphopeptide signal candidates for targeted LC- tandem MS analyses and subsequently assisted label-free quantitative tyrosine phosphoproteomics. We also demonstrated an application of the proposed alternative approach to further understand the signaling pathway of dasatinib-treated highly invasive CL1-5 lung cancer cells. Many of altered Src-associated proteins discovered here were regulated by transcription factor E2F1, one of the E2F family members that play a crucial role in the control of cell cycle and apoptosis. This indicated that dasatinib exhibited its Src inhibitory activity through E2F1 to affect the pTyr protein levels. We suggest ILT LC- tandem MS is a robust approach and plausible alternative to phosphopeptide enrichment with sufficient sensitivity for comprehensive label-free quantitative tyrosine phosphoproteomics.

Acknowledgement

The authors thank the National Cheng-Kung University Proteomics Research Core Laboratory for assistance in mass spectrometry analysis for protein identification. The study was supported by grants from the National Science Council of Taiwan (NSC 99-2923-M-006-001-MY3, NSC 100-2113-M-006-002-MY3, NSC 100-2325- B-006-004, and NSC 99-2628-B-006-015-MY3) and the National Cheng-Kung University Project of Promoting Academic Excellence & Developing World Class Research Centers from the Ministry of Education

of Taiwan. Proteomic LC-MS analyses and the label-free quantitative software, Progenesis LC-MS, were performed by the Core Facilities for Proteomics Research at the Institute of Biological Chemistry, Academia Sinica, supported by a National Science Council grant (NSC 98-3112-B-001-023, NSC 99-3112-B-001-025) and the Academia Sinica. Pathway analysis using MetaCore software was provided by the Bioinformatics Core for Genomic Medicine and Biotechnology Development at the National Cheng-Kung University, supported by a National Science Council grant (NSC97-3112-B-006-011).

References

1. Amanchy R, Periaswamy B, Mathivanan S, Reddy R, Tattikota SG, et al. (2007). A curated compendium of phosphorylation motifs. Nat Biotechnol, 25:285-6.
2. Barnouin KN, Hart SR, Thompson AJ, Okuyama M, Waterfield M, et al. (2005). Enhanced phosphopeptide isolation by Fe(III)-IMAC using 1,1,1,3,3,3-hexafluoroisopropanol. Proteomics, 5:4376-88.
3. Bergstrom Lind S, Molin M, Savitski MM, Emilsson L, Astrom J, et al. (2008). Immunoaffinity enrichments followed by mass spectrometric detection for studying global protein tyrosine phosphorylation. J Proteome Res, 7:2897-910.
4. Bieda M, Xu X, Singer MA, Green R, and Farnham PJ (2006). Unbiased location analysis of E2F1-binding sites suggests a widespread role for E2F1 in the human genome. Genome Res, 16:595-605.
5. Blume-Jensen P and Hunter T (2001). Oncogenic kinase signalling. Nature, 411:355-65.
6. Brill LM, Salomon AR, Ficarro SB, Mukherji M, Stettler-Gill M, et al. (2004). Robust phosphoproteomic profiling of tyrosine phosphorylation sites from human T cells using immobilized metal affinity chromatography and tandem mass spectrometry. Anal Chem, 76:2763-72.
7. Caccia D, Micciche F, Cassinelli G, Mondellini P, Casalini P, et al. (2010). Dasatinib reduces FAK phosphorylation increasing the effects of RPI-1 inhibition in a RET/PTC1-expressing cell line. Mol Cancer, 9:278.
8. Ceppi P, Papotti M, Monica V, Lo Iacono M, Saviozzi S, et al. (2009). Effects of Src kinase inhibition induced by dasatinib in non-small cell lung cancer cell lines treated with cisplatin. Mol Cancer Ther, 8:3066-74.
9. Chang YC, Lin SY, Liang SY, Pan KT, Chou CC, et al. (2008). Tyrosine phosphoproteomics and identification of substrates of protein tyrosine phosphatase dPTP61F in Drosophila S2 cells by mass spectrometry-based substrate trapping strategy. J Proteome Res, 7:1055-66.
10. Chen X, Xu H, Yuan P, Fang F, Huss M, et al. (2008). Integration of external signaling pathways with the core transcriptional network in embryonic stem cells. Cell, 133:1106-17.
11. Chiu KH, Chang YH, Wu YS, Lee SH, and Liao PC (2011). Quantitative secretome analysis reveals that COL6A1 is a metastasis-associated protein using stacking gel-aided purification combined with iTRAQ labeling. J Proteome Res, 10:1110-25.
12. Chu YW, Yang PC, Yang SC, Shyu YC, Hendrix MJ, et al. (1997). Selection of invasive and metastatic subpopulations from a human lung adenocarcinoma cell line. Am J Respir Cell Mol Biol, 17:353-60.
13. Emadali A, Metrakos PP, Kalantari F, Boutros T, Boismenu D, et al. (2007). Proteomic analysis of tyrosine phosphorylation during human liver transplantation. Proteome Sci, 5:1.
14. Ficarro SB, McCleland ML, Stukenberg PT, Burke DJ, Ross MM, et al. (2002). Phosphoproteome analysis by mass spectrometry and its application to Saccharomyces cerevisiae. Nat Biotechnol, 20:301-5.
15. Flirski M and Sobow T (2005). Biochemical markers and risk factors of Alzheimer's disease. Curr Alzheimer Res, 2:47-64.
16. Gembitsky DS, Lawlor K, Jacovina A, Yaneva M, and Tempst P (2004). A prototype antibody microarray

platform to monitor changes in protein tyrosine phosphorylation. Mol Cell Proteomics, 3:1102-18.

17. Gnad F, Gunawardena J, and Mann M (2011). PHOSIDA 2011: the posttranslational modification database. Nucleic Acids Res, 39:D253-60.
18. Gnad F, Ren S, Cox J, Olsen JV, Macek B, et al. (2007). PHOSIDA (phosphorylation site database): management, structural and evolutionary investigation, and prediction of phosphosites. Genome Biol, 8:R250.
19. Gnoni A, Marech I, Silvestris N, Vacca A, and Lorusso V (2011). Dasatinib: an anti-tumour agent via Src inhibition. Curr Drug Targets, 12:563-78.
20. Han G, Ye M, and Zou H (2008). Development of phosphopeptide enrichment techniques for phosphoproteome analysis. Analyst, 133:1128-38.
21. Hatzimanikatis V, Choe LH, and Lee KH (1999). Proteomics: theoretical and experimental considerations. Biotechnol Prog, 15:312-8.
22. Heibeck TH, Ding SJ, Opresko LK, Zhao R, Schepmoes AA, et al. (2009). An extensive survey of tyrosine phosphorylation revealing new sites in human mammary epithelial cells. J Proteome Res, 8:3852-61.
23. Hirai A, Tada M, Furuuchi K, Ishikawa S, Makiyama K, et al. (2004). Expression of AIE-75 PDZ-domain protein induces G2/M cell cycle arrest in human colorectal adenocarcinoma SW480 cells. Cancer Lett, 211:209-18.
24. Hornbeck PV, Kornhauser JM, Tkachev S, Zhang B, Skrzypek E, et al. (2012). PhosphoSitePlus: a comprehensive resource for investigating the structure and function of experimentally determined post-translational modifications in man and mouse. Nucleic Acids Res, 40:D261-70.
25. Hunter T (2000). Signaling--2000 and beyond. Cell, 100:113-27.
26. Iliuk AB, Martin VA, Alicie BM, Geahlen RL, and Tao WA (2010). In-depth analyses of kinase-dependent tyrosine phosphoproteomes based on metal ion-functionalized soluble nanopolymers. Mol Cell Proteomics, 9:2162-72.
27. Jaffe JD, Keshishian H, Chang B, Addona TA, Gillette MA, et al. (2008). Accurate inclusion mass screening: a bridge from unbiased discovery to targeted assay development for biomarker verification. Mol Cell Proteomics, 7:1952-62.
28. Jin VX, Rabinovich A, Squazzo SL, Green R, and Farnham PJ (2006). A computational genomics approach to identify cis-regulatory modules from chromatin immunoprecipitation microarray data--a case study using E2F1. Genome Res, 16:1585-95.
29. Keshava Prasad TS, Goel R, Kandasamy K, Keerthikumar S, Kumar S, et al. (2009). Human Protein Reference Database--2009 update. Nucleic Acids Res, 37:D767-72.
30. Lapierre LA, Avant KM, Caldwell CM, Ham AJ, Hill S, et al. (2007). Characterization of immunoisolated human gastric parietal cells tubulovesicles: identification of regulators of apical recycling. Am J Physiol Gastrointest Liver Physiol, 292:G1249-62.
31. Larsen MR, Thingholm TE, Jensen ON, Roepstorff P, and Jorgensen TJ (2005). Highly selective enrichment of phosphorylated peptides from peptide mixtures using titanium dioxide microcolumns. Mol Cell Proteomics, 4:873-86.
32. Lemeer S, Kunold E, Klaeger S, Raabe M, Towers MW, et al. (2012). Phosphorylation site localization in peptides by MALDI MS/MS and the Mascot Delta Score. Anal Bioanal Chem, 402:249-60.
33. Liao PC, Leykam J, Andrews PC, Gage DA, and Allison J (1994). An approach to locate phosphorylation sites in a phosphoprotein: mass mapping by combining specific enzymatic degradation with matrix-assisted laser desorption/ionization mass spectrometry. Anal Biochem, 219:9-20.
34. Lim YP (2005). Mining the tumor phosphoproteome for cancer markers. Clin Cancer Res, 11:3163-9.
35. Machida K, Mayer BJ, and Nollau P (2003). Profiling the global tyrosine phosphorylation state. Mol Cell

Proteomics, 2:215-33.

36. Marcantonio M, Trost M, Courcelles M, Desjardins M, and Thibault P (2008). Combined enzymatic and data mining approaches for comprehensive phosphoproteome analyses: application to cell signaling events of interferon-gamma-stimulated macrophages. Mol Cell Proteomics, 7:645-60.
37. Montero JC, Seoane S, Ocana A, and Pandiella A (2011). Inhibition of SRC family kinases and receptor tyrosine kinases by dasatinib: possible combinations in solid tumors. Clin Cancer Res, 17:5546-52.
38. Nishiyama A, Xin L, Sharov AA, Thomas M, Mowrer G, et al. (2009). Uncovering early response of gene regulatory networks in ESCs by systematic induction of transcription factors. Cell Stem Cell, 5:420-33.
39. Olsen JV, Blagoev B, Gnad F, Macek B, Kumar C, et al. (2006). Global, in vivo, and site-specific phosphorylation dynamics in signaling networks. Cell, 127:635-48.
40. Ostman A and Bohmer FD (2001). Regulation of receptor tyrosine kinase signaling by protein tyrosine phosphatases. Trends Cell Biol, 11:258-66.
41. Pearce LR, Komander D, and Alessi DR (2010). The nuts and bolts of AGC protein kinases. Nat Rev Mol Cell Biol, 11:9-22.
42. Phillips RM, Burger AM, Fiebig HH, and Double JA (2001). Genotyping of NAD(P)H:quinone oxidoreductase (NQO1) in a panel of human tumor xenografts: relationship between genotype status, NQO1 activity and the response of xenografts to Mitomycin C chemotherapy in vivo(1). Biochem Pharmacol, 62:1371-7.
43. Pinna LA and Ruzzene M (1996). How do protein kinases recognize their substrates? Biochim Biophys Acta, 1314:191-225.
44. Premkumar DR, Jane EP, Agostino NR, Scialabba JL, and Pollack IF (2010). Dasatinib synergizes with JSI-124 to inhibit growth and migration and induce apoptosis of malignant human glioma cells. J Carcinog, 9.
45. Rikova K, Guo A, Zeng Q, Possemato A, Yu J, et al. (2007). Global survey of phosphotyrosine signaling identifies oncogenic kinases in lung cancer. Cell, 131:1190-203.
46. Rush J, Moritz A, Lee KA, Guo A, Goss VL, et al. (2005). Immunoaffinity profiling of tyrosine phosphorylation in cancer cells. Nat Biotechnol, 23:94-101.
47. Ryu B, Kim DS, Deluca AM, and Alani RM (2007). Comprehensive expression profiling of tumor cell lines identifies molecular signatures of melanoma progression. PLoS One, 2:e594.
48. Salomon AR, Ficarro SB, Brill LM, Brinker A, Phung QT, et al. (2003). Profiling of tyrosine phosphorylation pathways in human cells using mass spectrometry. Proc Natl Acad Sci U S A, 100:443-8.
49. Savitski MM, Lemeer S, Boesche M, Lang M, Mathieson T, et al. (2011). Confident phosphorylation site localization using the Mascot Delta Score. Mol Cell Proteomics, 10:M110 003830.
50. Schmidt A, Gehlenborg N, Bodenmiller B, Mueller LN, Campbell D, et al. (2008). An integrated, directed mass spectrometric approach for in-depth characterization of complex peptide mixtures. Mol Cell Proteomics, 7:2138-50.
51. Schumacher JA, Crockett DK, Elenitoba-Johnson KS, and Lim MS (2007). Evaluation of enrichment techniques for mass spectrometry: identification of tyrosine phosphoproteins in cancer cells. J Mol Diagn, 9:169-77.
52. Sugiyama N, Masuda T, Shinoda K, Nakamura A, Tomita M, et al. (2007). Phosphopeptide enrichment by aliphatic hydroxy acid-modified metal oxide chromatography for nano-LC-MS/MS in proteomics applications. Mol Cell Proteomics, 6:1103-9.
53. Taus T, Kocher T, Pichler P, Paschke C, Schmidt A, et al. (2011). Universal and confident phosphorylation site localization using phosphoRS. J Proteome Res,

10:5354-62.

54. Trinkle-Mulcahy L, Andersen J, Lam YW, Moorhead G, Mann M, et al. (2006). Repo-Man recruits PP1 gamma to chromatin and is essential for cell viability. J Cell Biol, 172:679-92.
55. Vagnarelli P, Hudson DF, Ribeiro SA, Trinkle-Mulcahy L, Spence JM, et al. (2006). Condensin and Repo-Man-PP1 co-operate in the regulation of chromosome architecture during mitosis. Nat Cell Biol, 8:1133-42.
56. Verma NK, Dempsey E, Freeley M, Botting CH, Long A, et al. (2011). Analysis of dynamic tyrosine phosphoproteome in LFA-1 triggered migrating T-cells. J Cell Physiol, 226:1489-98.
57. Wang YT, Tsai CF, Hong TC, Tsou CC, Lin PY, et al. (2010). An informatics-assisted label-free quantitation strategy that depicts phosphoproteomic profiles in lung cancer cell invasion. J Proteome Res, 9:5582-97.
58. Wolf-Yadlin A, Hautaniemi S, Lauffenburger DA, and White FM (2007). Multiple reaction monitoring for robust quantitative proteomic analysis of cellular signaling networks. Proc Natl Acad Sci U S A, 104:5860-5.
59. Wu HY, Tseng VS, and Liao PC (2007). Mining phosphopeptide signals in liquid chromatography-mass spectrometry data for protein phosphorylation analysis. J Proteome Res, 6:1812-21.
60. Wu HY, Tseng VS, Chen LC, Chang HY, Chuang IC, et al. (2010). Identification of tyrosine-phosphorylated proteins associated with lung cancer metastasis using label-free quantitative analyses. J Proteome Res, 9:4102-12.
61. Wu HY, Tseng VS, Chen LC, Chang YC, Ping P, et al. (2009). Combining alkaline phosphatase treatment and hybrid linear ion trap/Orbitrap high mass accuracy liquid chromatography-mass spectrometry data for the efficient and confident identification of protein phosphorylation. Anal Chem, 81:7778-87.